Efficient encapsulation with plug-triggered drop formation

Adam R. Abate,[1,*] Assaf Rotem,[1] Julian Thiele,[2] and David A. Weitz[1]
[1]*Department of Physics, School of Engineering and Applied Sciences, Harvard University, Cambridge, Massachusetts 02138, USA*
[2]*Institute of Physical Chemistry, University of Hamburg, Hamburg 20146, Germany*
(Received 22 January 2011; revised manuscript received 14 June 2011; published 22 September 2011)

Monodisperse microscale drops formed with microfluidic devices are useful for encapsulating cells, microgel particles, or even additional drops. These techniques are thus useful for applications ranging from high-throughput biology to monodisperse particle and capsule synthesis, which require encapsulation of such objects. However, it is challenging to efficiently encapsulate the objects in all drops; often, the objects are encapsulated inefficiently, resulting in many improperly filled, unusable drops. Here, we describe a phenomenon that allows very efficient encapsulation. We use the inflow of the object to plug the drop maker nozzle; the continued injection of the outer phase pinches off a drop, thereby encapsulating the object; this yields precisely one object encapsulated per drop.

DOI: 10.1103/PhysRevE.84.031502 PACS number(s): 83.80.Qr, 83.50.−v, 47.20.Ma, 47.15.Rq

I. INTRODUCTION

Microfluidic devices can form monodisperse drops with controlled properties and dimensions [1–4]. They can also load objects in the drops, including cells, microgel particles, and even additional drops [5–8]. These techniques are attractive for applications in high-throughput biology: Using drops as tiny "test tubes," cells, beads, and other reagents can be encapsulated to perform large numbers of reactions at high rates, for ultraefficient directed evolution, and genetic sequencing applications [9–13]. These techniques are also attractive for microstructure synthesis: By loading microgels or small drops in the drops, nonspherical Janus particles, anisotropic hydrogels, and polymersome vesicles can be created [14–19]. However, a challenge when using microfluidics for these applications is achieving controlled, efficient encapsulation of the objects; often, the objects are encapsulated in an uncontrolled process, resulting in a large fraction of improperly filled drops. In high-throughput biology applications, this reduces speed and efficiency; in material synthesis, it degrades the quality of the product.

One way to increase encapsulation efficiency is to order the objects so that they flow at regular rates; by synchronizing this with drop formation, higher encapsulation efficiency can be achieved. For small objects like particles or cells, ordering can be accomplished by flowing at high velocities so that inertial effects become important; this creates wakes in the flow around the particles, generating interactions that cause them to arrange into a regular spacing, thereby producing regular flow [20]. Alternatively, deformable objects like cells, microgels, or drops can be ordered using close-packing forces; the objects are introduced into a device at high volume fraction, inducing packing forces that cause the particles to order into a crystalline array, again leading to regular particle flow [8]. In both techniques, the final step for achieving efficient encapsulation is synchronizing the object flow with the drop formation, typically accomplished by adjusting flow rates [7,19]. However, the precision with which flow rates can be adjusted is limited, resulting in some asynchronicity, and repeated cycles of poor encapsulation. Moreover, even for ideal settings, pumps are limited in their ability to maintain steady flow, resulting in small variations in flow conditions, and again leading to intervals of poor encapsulation. For much higher encapsulation efficiencies to be achieved, a technique that can passively synchronize object flow with drop formation, even through fluctuations in flow, is needed.

In this paper, we describe a phenomenon that passively synchronizes these events: We use the inflow of an object to trigger the formation of a droplet. We introduce the objects into a drop maker device having a nozzle that is long and narrow; when the object is in the nozzle, and in the optimal position for encapsulation, it creates a temporary plugging that causes the pressure to rise in the continuous phase upstream; this induces droplet pinch off. The resultant drop contains the object inside. Drops only form when objects are present, yielding exactly one object encapsulated per drop, even through fluctuations in object periodicity of up to 50%.

II. TRIGGERING DROP FORMATION WITH DISCRETE REAGENTS

The triggered drop maker consists of a cross-channel junction with a long and narrow nozzle channel, having dimensions comparable to those of the objects, as illustrated in Fig. 1. When an object is in the nozzle, this allows it to plug the channel, restricting the path of the continuous phase, and causing the pressure to rise upstream. The increased pressure makes the continuous phase squeeze on the dispersed phase, causing the dispersed phase to narrow, pinching off into a drop with the object encapsulated inside. In this way, the object triggers the formation of the drop when in the optimal position for being encapsulated, as illustrated in Fig. 1.

To illustrate the basic principles of this process, we use a triggered drop maker with cross-sectional dimensions approximately the same size as that of the object to be encapsulated. The device is fabricated in poly(dimethylsiloxane) (PDMS) using soft lithography [21]. To trigger the drop formation in this experiment, we use small oil drops produced in a cross junction upstream of the triggering junction [5,17]; the final product of this device is a double emulsion, in which the small drops are encapsulated within the triggered drops.

To enable double emulsification, the wettability of the device is also spatially patterned: Using flow-controlled chemical

*adam.abate@ucsf.edu

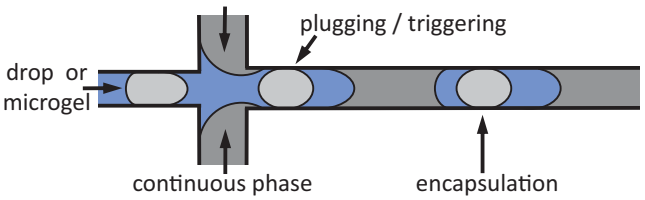

FIG. 1. (Color online) Schematic of triggered drop formation device. Drops or microgels are introduced into the inner phase inlet of the device and the continuous phase from two side inlets; when the objects enter the nozzle, they plug it, triggering drop formation. The objects should be slightly deformable, allowing them to plug the nozzle without clogging it.

patterning and lithographic polymer grafting, we make the first cross junction hydrophilic and the second hydrophobic; this allows production of small oil drops surrounded by water in the first drop maker, which trigger formation of large water drops surrounded by oil in the second drop maker [22,23]. As fluids for the double emulsion, we use HFE-7500 fluorocarbon oil for the small drop, water with sodium dodecyl sulfate (SDS) at 0.5 wt% for the triggered drop, and HFE-7500 fluorocarbon oil for the continuous phase; in the continuous phase, we use the ammonium salt of Krytox 157 FSL as surfactant, dissolved at 1.8 wt%. These fluids are injected into the inner, middle, and outer phase inlets of the device, at 200, 550, and 400 μl/h, respectively.

To visualize the dynamics during the triggering process, we image the triggering junction at high magnification and record movies with a fast camera, an image sequence from which is shown in Fig. 2; the full movie is available in the Supplemental Material accompanying this paper [24]. The double emulsions are composed of inner drops of fluorocarbon oil, encapsulated in a middle phase of water containing 1-μm polystyrene tracer particles, surrounded by a continuous phase of fluorocarbon oil with the Krytox surfactant. Early in the drop formation cycle, a bulge of the middle phase extends into the nozzle, as shown in $t = 0$ and 0.24 ms in Fig. 2. If the inner drop were not present, this fluid would immediately pinch into a drop; however, the inner drop interferes with this process, preventing immediate drop formation. Instead, the middle-phase interface narrows in an attempt to form a drop, but encounters the inner drop; due to the Laplace pressure of the inner drop, it is able to resist the pinching. The magnitudes of the forces competing in this process can be estimated from the Laplace pressures of the liquids. The inner drop has a radius of curvature of $\sim$12 μm, corresponding to a Laplace pressure of $\Delta P = 2\sigma/r =$ 0.7 kPa. The inward squeezing of the middle phase interface can be estimated by calculating the pressure difference between the narrowest part of the pinch and the bulges on either side; the pinch has a radius of curvature of 12 μm and the bulges 13 μm, producing a squeezing pressure of $\sim$0.05 kPa. Thus, the squeezing pressure is over an order of magnitude smaller than the Laplace pressure of the inner drop, allowing the inner drop to resist the pinching; instead, the inner drop continues down the nozzle without being pinched in two, as shown for $t = 0.72$ ms in Fig. 2. The inner drop plugs the nozzle, causing the pressure to rise in the continuous phase

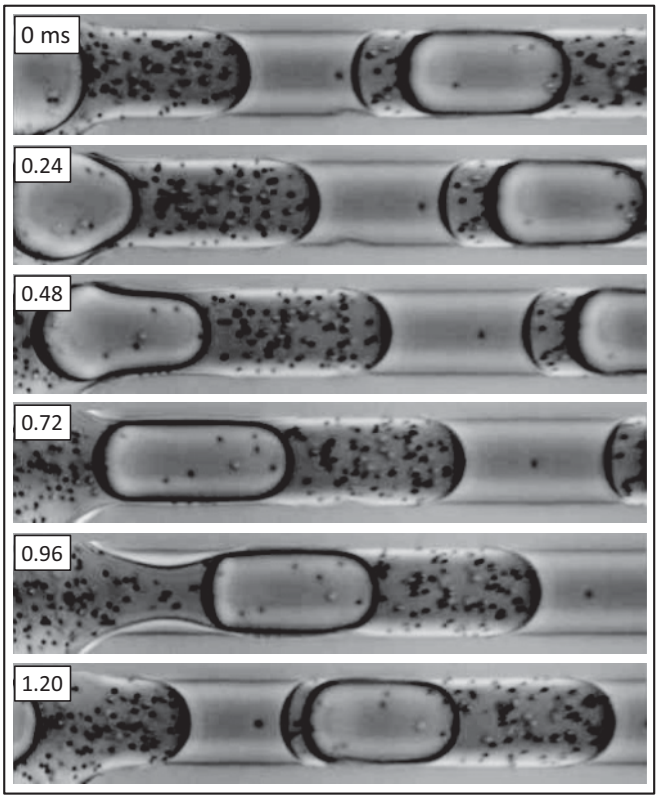

FIG. 2. Image sequence of a small drop triggering the formation of a large drop. For the small drop to fit in the nozzle, it must distort from a spherical shape to a sausage shape; this allows it to plug the nozzle, restricting the path of the continuous phase, causing a pressure rise upstream that induces pinch off of a large drop. The channel width is 25 μm. Movies of the process are available in the Supplemental Material [24].

upstream, which is now restricted to flow through gutters at the corners of the channel and thin lubricating layers on its faces. This causes the continuous phase to squeeze on the middle phase, creating a narrow bridge of fluid behind the inner drop, as shown for $t = 0.96$ ms in Fig. 2. When the bridge is reduced to a sufficiently narrow width, it becomes unstable due to the Rayleigh-Plateau instability, snapping, and producing a double emulsion, as shown for $t = 1.2$ ms in Fig. 2.

III. DEPENDENCE ON TRIGGERING OBJECT SIZE

For triggering to occur, the size of the inner object is crucial, because it must be sufficiently large to plug the nozzle leading to the cascade of events that culminate with pinch off. To investigate the importance of inner drop size, we construct a device that allows us to vary drop size at fixed flow rates. This device is another double cross-junction device, though this time the first junction is outfitted with single-layer membrane valves, as illustrated in Fig. 3(a); these allow us to adjust the dimensions of the first junction, to change inner drop size while maintaining constant flow rates, in a process known as valve-based flow focusing [25].

We begin with the nozzle constricted, producing small drops. These enter the second junction, where the outer drops are formed. Because the inner drops are small, they cannot

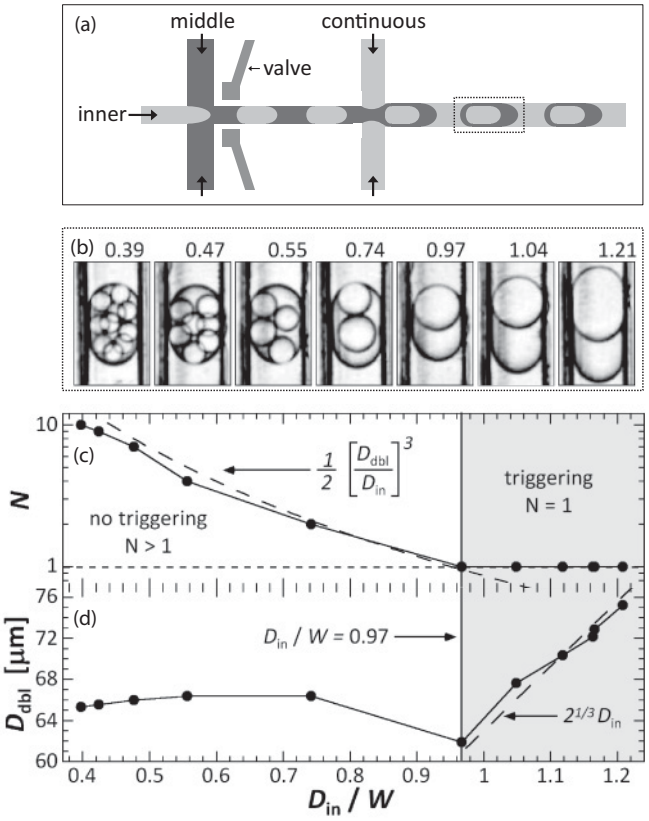

FIG. 3. Dependence of triggering on inner drop size. (a) Schematic of valve-based flow focusing device for making double emulsions; using the valves, the inner drop size can be varied while maintaining constant flow rates in the triggering junction. (b) Images of double emulsions formed with different inner drop sizes. (c) The number of inner drops encapsulated per outer drop and (d) the size of the entire double emulsion as a function of the inner drop diameter divided by the channel width. When the inner drop is smaller than the nozzle, triggering does not occur; the number encapsulated is inversely proportional to inner drop size and the double emulsion diameter is roughly constant. By contrast, when the inner drop is larger than the nozzle, drop formation is triggered; every outer drop contains exactly one inner drop, and the size of the double emulsion scales with that of the inner drops.

plug the nozzle, and thus do not trigger drop formation; consequently, the outer drops form independently of the inner drops, leading to several inner drops encapsulated per outer drop, as shown in Figs. 3(b) and 3(c) (left). As we relax the pressure on the valves, we widen the first nozzle, producing bigger inner drops; however, they are still too small to trigger drop formation, leading to fewer, though still several, inner drops encapsulated, as shown in Figs. 3(b) and 3(c) (middle left). In this state, the formations of the inner and outer drops are independent, though both processes are periodic; as a consequence, the number of inner drops encapsulated depends on the relative frequencies of both drop formations. If the inner drop frequency is an integer multiple of the outer drop and both are in phase, then a uniform number of inner drops will be encapsulated; however, this is almost never the case, and instead the number encapsulated varies from one double emulsion to the next, as the drop formation frequencies beat in and out of phase. Because the flow rates are fixed in these experiments, the average number of inner drops encapsulated can be predicted using volume conservation, assuming that the formation of the outer drops is independent from that of the inner drops; in this case, the number encapsulated is proportional to the flow rate ratio, and thus the ratio of the volume of the double emulsion to that of the inner drops, as shown by comparison of our data with the prediction (dashed line) in Fig. 3(c) (left). In this regime when drop formation is not triggered, the diameter of the double emulsions is approximately constant, because the size at which the outer drops form is determined by the flow conditions in the second nozzle, which are unchanged by actuating the valves, as shown in Fig. 3(d) (left). By contrast, if inner drop size is increased to become comparable to that of the nozzle, there is an abrupt switch in the behavior: Rather than several inner drops encapsulated only one is encapsulated, as shown in Figs. 3(b) and 3(c) (right). Moreover, the outer drop formation is no longer independent of that of the inner drops; an outer drop forms only when triggered by an inner drop. Changing inner drop size leads to proportional change in the total double emulsion size, as shown in Fig. 3(d) (right). This distinct behavior can be explained through the triggering. For fixed flow rates, the double emulsion size depends on the trigger rate, which determines how long the middle phase has to fill; if inner drop size is increased, the trigger rate decreases because the inner drops take longer to form. This allows the outer drop to inflate for a longer period before being triggered, resulting in proportionally larger double emulsions, as shown by comparison with the prediction (dashed curve) in Fig. 3(d) (right).

IV. SCALING OF DROP SIZE

These experiments demonstrate that when triggering applies, the properties of drop formation are different compared to usual drop formation, leading to distinct scaling. To demonstrate that, indeed, the drop formation properties do change, we compare measurements of drop size as a function of flow conditions with three potentially applicable scenarios. The first scenario we consider is shearing drop formation, which accurately predicts scaling of drop size in microfluidic coflow drop makers [1,26,27]. These drop makers have the property that the microchannel walls are relatively far from the point of drop formation, so that the continuous phase can be treated as unbounded. In this scenario, the growing bulge of the drop is assumed to be sheared by the flow of the continuous phase rushing over it; this imposes a viscous drag that scales with the size of the bulge. When the bulge increases to a critical size, the drag force exceeds the surface tension force adhering it to the inlet, ripping off a drop. This yields that the drop size scale with the inverse of the continuous phase capillary number (Ca); however, our data do not collapse as a function of $1/\mathrm{Ca}$; moreover, the scaling is incorrect, as shown in Fig. 4(a). The failure of this scenario is not surprising because it assumes unbounded continuous phase flow; by contrast, in our cross junction the flows are highly confined.

An alternative scenario that includes confinement is plugging drop formation [4,28]. Within this picture drops form due to fluctuating pressures in the continuous phase. The protruding tip of the dispersed phase plugs the nozzle,

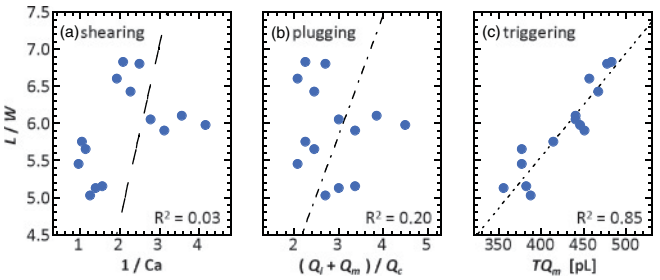

FIG. 4. (Color online) Comparison of our data with three potentially applicable drop formation scenarios. The plots show the measured drop lengths divided by the channel width, as a function of control parameters relevant to the scenarios. (a) Shear-driven drop formation predicts scaling with the inverse of the Ca of the continuous phase. (b) Plugging drop formation predicts scaling with the flow rate ratio of the inner and middle phases, with respect to the continuous phase. (c) Plug-triggered drop formation predicts scaling with the triggering period times the middle phase flow rate. While our data neither collapse nor scale as predicted when compared with shear-driven or plugging drop formation, they do when compared with plug-triggered drop formation.

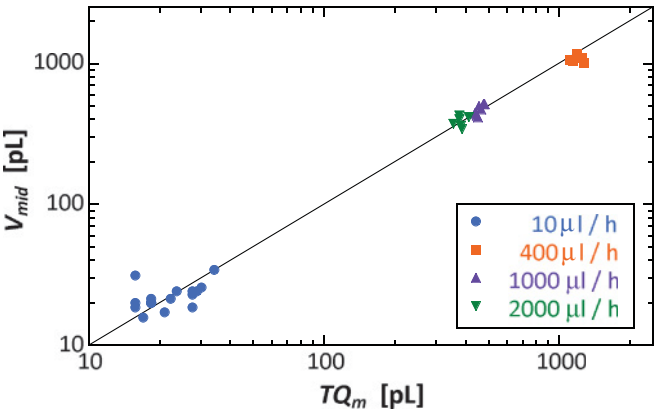

FIG. 5. (Color online) Scaling of middle-phase drop volumes with the triggering control parameter TQ_m. Each drop is composed of a volume of middle phase V_{mid} in which an object is encapsulated, so that the total volume $V_{\text{drop}} = V_{\text{mid}} + V_{ob}$, where V_{ob} is the object volume. Increasing the middle phase flow rate Q_m or the triggering period T, both lead to a proportional increase in the V_{mid}. The solid line shows the scaling expected for triggering, in which $V_{\text{mid}} = TQ_m$.

restricting the flow of the continuous phase; this causes the continuous phase pressure to increase, so that it squeezes on the dispersed phase. This leads to the development of a narrow thread of fluid behind the tip of the emerging drop, which eventually snaps, producing a drop. This suggests that the drop volume scales with the flow rate ratio of the inner-to-middle phase, $V = Lw^2[1 - \alpha(Q_i + Q_m)]/Q_c$; here, L and w are the drop length and width, α is a geometrical parameter close to 1, and Q_i, Q_m, and Q_c are the inner, middle, and continuous phase flow rates, respectively. When plotted as a function of $(Q_i + Q_m)/Q_c$, however, our data again do not collapse; nor do they exhibit the proper scaling, as shown in Fig. 4(b).

To account for the observed behavior, we assume that the plugging of the nozzle is accomplished by the inner drop, and not by the tip of the outer drop; consequently, drops form only when the inner drops are present to trigger them, leading to a simple linear scaling for drop volume, $V = TQ_m$, where V is the drop volume not including the object volume, T is the trigger rate, and Q_m is the middle phase flow rate. Longer trigger times or higher middle phase flow rates lead to large drops; consistent with this, as a function of TQ_m our data collapse and exhibit the correct scaling, as shown in Fig. 4(c).

To further confirm this scenario, we extend our measurements over a wider range of TQ_m; we accomplish this using both microgel particles and small drops to trigger drop formation. All data again collapse when plotted as a function of TQ_m and exhibit the predicted scaling, as shown in Fig. 5. This demonstrates that the process is the same whether microgels or drops are used to trigger drop formation; moreover, drop size can be controlled by modulating triggering times and flow rates.

V. TRIGGERING WITH MICROGELS

Triggering can compensate for variations in object periodicity, to maintain high encapsulation efficiency even when pumping rates vary. This is useful because all pumps are limited in precision, and so in practice triggering affords higher encapsulation efficiency. Nevertheless, triggering has its limits and cannot compensate for extreme variations in flow rate. To quantify these limits, we vary the object periodicity and determine the extent to which triggering can compensate. We trigger drop formation using microgels, introduced into a double cross-channel junction, as shown in images of the device in Fig. 6(a). The microgels are made using droplet-based particle templating [29]. The microgels enter from the

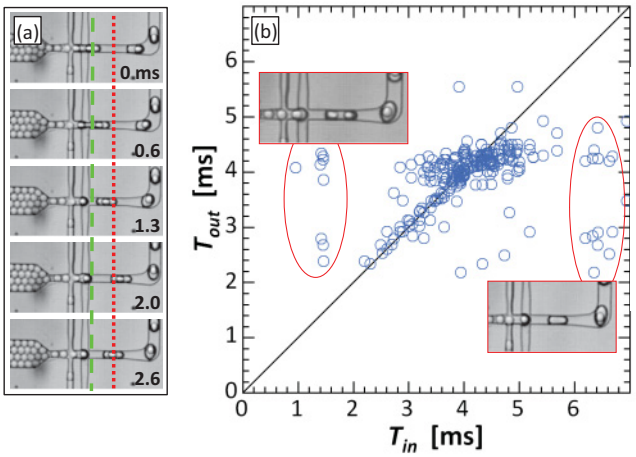

FIG. 6. (Color online) Analysis of when triggering fails. (a) Image sequence of microgel-triggered drop formation; the green dashed line and red dotted line correspond to the locations at which the microgel and drop intervals, respectively, are measured. (b) The drop formation interval as a function of the microgel interval; for triggered drop formation, these intervals must be equal, so that there is a linear dependence between them with a slope of unity, which is what we observe for a majority of drops. However, occasionally microgels enter too quickly so that two are encapsulated, or too slowly so that empty drops are formed. For drop formation to be successfully triggered, the object frequency must be within ~50% of the natural drop formation frequency of the device.

far left as a dense pack and are spaced by addition of water from two side channels; they then enter the triggering junction, where they are encapsulated in water drops surrounded by fluorocarbon oil, as shown in Fig. 6(a). To cause the trigger rate to vary, we add an abrupt constriction to the microgel inlet; this allows the microgels to occasionally form arches at the constriction, causing a temporary jam that leads to irregular particle flow [8]. We measure the interval between consecutive microgels as they pass the green dashed line and also the interval between fully formed drops as they pass the red dotted line, both shown in Fig. 6(a). For correctly triggered drops, these intervals should be equal, and we expect a linear dependence with slope of unity; this, indeed, is what we observe for a majority of drops, as shown in Fig. 6(b). Nevertheless, there are occasions when the intervals are not equal; these represent times when triggering fails: In the first category, two microgels enter in rapid succession so that the interval is shorter than the time necessary for the drop to pinch off after the passage of the first microgel; instead, the drop does not pinch and the two microgels are encapsulated in one drop, as shown in Fig. 6(b) (upper left). In the second category, the interval between microgels is long, because of a jam in the inlet; over this time, the middle phase continues to flow into the nozzle and the system behaves like a typical cross-channel drop maker, forming an empty drop with no microgels, as shown in Fig. 6(b) (lower right). For triggering to be effective, the object and drop interval must thus not be too different. From our measurements, we estimate that variations of up to 50% in the intervals can be compensated.

VI. DISCUSSION

Triggering is an effective way to efficiently encapsulate objects in drops, while forming monodisperse drops of controlled size. It requires only that the objects be of a comparable size to the drop formation nozzle, and that object flow be roughly periodic and of a similar frequency to that of the drop formation. In this state, even if the drop and object frequencies vary, triggering ensures that the two events remain synchronized, for exactly one object encapsulated in every drop. The simplicity, passive nature, and ability of this technique to compensate for imperfections in pumps and irregularities in flow should make it of general use for applications requiring exceedingly high encapsulation efficiency, including for high-throughput biology applications requiring encapsulation of cells and microgels, and particle or capsule synthesis requiring encapsulation of drops and other compliant objects.

ACKNOWLEDGMENTS

This work was supported by the NSF (Grant No. DMR-1006546), the Harvard MRSEC (Grant No. DMR-0820484), and the Massachusetts Life Sciences Center. J.T. thanks the Fund of the Chemical Industry (Germany) for financial support.

[1] P. B. Umbanhowar, V. Prasad, and D. A. Weitz, Langmuir **16**, 347 (2000).
[2] T. Thorsen, R. W. Roberts, F. H. Arnold, and S. R. Quake, Phys. Rev. Lett. **86**, 4163 (2001).
[3] S. L. Anna, N. Bontoux, and H. A. Stone, Appl. Phys. Lett. **82**, 364 (2003).
[4] P. Garstecki, M. J. Fuerstman, H. A. Stone, and G. M. Whitesides, Lab Chip **6**, 437 (2006).
[5] T. Nisisako, S. Okushima, and T. Torii, Soft Matter **1**, 23 (2005).
[6] J. Clausell-Tormos, D. Lieber, J. C. Baret, A. El-Harrak, O. J. Miller, L. Frenz, J. Blouwolff, K. J. Humphry, S. Koster, H. Duan, C. Holtze, D. A. Weitz, A. D. Griffiths, and C. A. Merten, Chem. Biol. **15**, 427 (2008).
[7] J. F. Edd, D. Di Carlo, K. J. Humphry, S. Koster, D. Irimia, D. A. Weitz, and M. Toner, Lab-on-a-Chip **8**, 1262 (2008).
[8] A. R. Abate, C. H. Chen, J. J. Agresti, and D. A. Weitz, Lab Chip **9**, 2628 (2009).
[9] B. T. Kelly, J. C. Baret, V. Taly, and A. D. Griffiths, Chem. Commun. **14**, 1773 (2007).
[10] V. Taly, B. T. Kelly, and A. D. Griffiths, ChemBioChem **8**, 263 (2007).
[11] F. Courtois, L. F. Olguin, G. Whyte, D. Bratton, W. T. Huck, C. Abell, and F. Hollfelder, ChemBioChem **9**, 439 (2008).
[12] A. Huebner, L. F. Olguin, D. Bratton, G. Whyte, W. T. Huck, A. J. de Mello, J. B. Edel, C. Abell, and F. Hollfelder, Anal. Chem. **80**, 3890 (2008).
[13] J. J. Agresti, E. Antipov, A. R. Abate, K. Ahn, A. C. Rowat, J. C. Baret, M. Marquez, A. M. Klibanov, A. D. Griffiths, and D. A. Weitz, Proc. Natl. Acad. Sci. USA **107**, 4004 (2010).
[14] E. Lorenceau, A. S. Utada, D. R. Link, G. Cristobal, M. Joanicot, and D. A. Weitz, Langmuir **21**, 9183 (2005).
[15] A. S. Utada, E. Lorenceau, D. R. Link, P. D. Kaplan, H. A. Stone, and D. A. Weitz, Science **308**, 537 (2005).
[16] Z. H. Nie, W. Li, M. Seo, S. Q. Xu, and E. Kumacheva, J. Am. Chem. Soc. **128**, 9408 (2006).
[17] A. R. Abate and D. A. Weitz, Small **5**, 2030 (2009).
[18] C. H. Chen, R. K. Shah, A. R. Abate, and D. A. Weitz, Langmuir **25**, 4320 (2009).
[19] S. Seiffert, J. Thiele, A. R. Abate, and D. A. Weitz, J. Am. Chem. Soc. **132**, 6606 (2010).
[20] D. Di Carlo, D. Irimia, R. G. Tompkins, and M. Toner, Proc. Natl. Acad. Sci. USA **104**, 18892 (2007).
[21] Y. Xia and G. M. Whitesides, Angew. Chem., Int. Ed. Engl. **37**, 550 (1998).
[22] A. R. Abate, A. T. Krummel, D. Lee, M. Marquez, C. Holtze, and D. A. Weitz, Lab Chip **8**, 2157 (2008).
[23] A. R. Abate, J. Thiele, M. Weinhart, and D. A. Weitz, Lab Chip **10**, 1774 (2010).
[24] See Supplemental Material at http://link.aps.org/supplemental/10.1103/PhysRevE.84.031502 for fast-camera movies of triggered drop formation.
[25] A. R. Abate, M. B. Romanowsky, J. J. Agresti, and D. A. Weitz, Appl. Phys. Lett. **94**, 023503 (2009).
[26] A. S. Utada, A. Fernandez-Nieves, H. A. Stone, and D. A. Weitz, Phys. Rev. Lett. **99**, 094502 (2007).
[27] A. S. Utada, A. Fernandez-Nieves, J. M. Gordillo, and D. A. Weitz, Phys. Rev. Lett. **100**, 014502 (2008).
[28] P. Guillot and A. Colin, Phys. Rev. E **72**, 066301 (2005).
[29] J. W. Kim, A. S. Utada, A. Fernandez-Nieves, Z. Hu, and D. A. Weitz, Angew. Chem. Int. Ed. Engl. **46**, 1819 (2007).